PCCP

Accepted Manuscript

ROYAL SOCIETY OF CHEMISTRY

www.rsc.org/pccp

Physical Chemistry Chemical Physics
CREATED USING THE RSC LaTeX PCCP ARTICLE TEMPLATE – SEE www.rsc.org/electronicfiles FOR DETAILS
ARTICLE TYPE www. rsc.org/xxxxxx | XXXXXXXX

Van der Waals density functionals applied to corundum-type sesquioxides: bulk properties and adsorption of CH_3 and C_6H_6 on (0001) surfaces

Samira Dabaghmanesh,*[a,b] Erik C. Neyts,[b] and Bart Partoens[a]

Van der Waals (vdW) forces play an important role in the adsorption of molecules on the surface of solids. However, the choice of the most suitable vdW functional for different systems is an essential problem which must be addressed for different systems. The lack of a systematic study on the performance of the vdW functionals in the bulk and adsorption properties of metal-oxides motivated us to examine different vdW approaches and compute bulk and molecular adsorption properties of α-Cr_2O_3, α-Fe_2O_3, and α-Al_2O_3. For the bulk properties, we compared our results for the heat of formation, cohesive energy, lattice parameters and bond distances between the different vdW functionals and available experimental data. Next we studied the adsorption of benzene and CH_3 molecules on top of different oxide surfaces. We employed different approximations to exchange and correlation within DFT, namely, the Perdew-Burke-Ernzerhof (PBE) GGA, (PBE)+U, and vdW density functionals [DFT(vdW-DF/DF2/optPBE/optB86b/optB88)+U] as well as DFT-D2/D3(+U) methods of Grimme for the bulk calculations and optB86b-vdW(+U) and DFT-D2(+U) for the adsorption energy calculations. Our results highlight the importance of vdW interactions not only in the adsorption of molecules, but, importantly also for the bulk properties. Although the vdW contribution in the adsorption of CH_3 (as a chemisorption interaction) is less important compared to the adsorption of benzene (as a physisorption interaction), this contribution is not negligible. Also adsorption of benzene on ferryl/chromyl terminated surfaces shows an important chemisorption contribution in which the vdW interactions becomes less significant.

1 Introduction

Density functional theory (DFT) is currently the most widely used approach to describe the electronic structure of materials. Despite major advantages brought by DFT, it has also resulted in major challenges, for example in the correct description of systems in which dispersion forces play an important role. The challenge is to accurately describe the exchange and correlation interactions. In the adsorption of atoms and molecules on the surface of solids the Van der Waals (vdW) interactions play an important role. This role becomes more significant whenever the vdW forces dominate the covalent interatomic interactions. Although this is well known, the contribution of vdW interactions is absent in popular DFT exchange correlation functionals, both in the local density approximation (LDA) and the generalized gradient approximation(GGA).

In last decade, developing approaches that include the contribution of vdW forces has been an important field of research in both chemistry and physics communities [1–5]. However, the choice of the most efficient vdW functional for different systems is still an open question. There exist several studies pertinent to the adsorption of weakly interacting molecules, such as benzene, water and noble gases, on metal surfaces [6–9] and phenol adsorption on graphite (0001) [10] as well as chemisorption examples, adsorption of phenol on α-Al_2O_3 [10] and glycine on Cr_2O_3 surfaces [11]. In these studies the inclusion of vdW forces resulted in enhanced adsorption energies and better agreement with experimental data. Currently, however, there are no systematic works pertinent to the role of vdW interactions in the bulk and adsorption properties of metal-oxides, and examining the performance of the recent developed vdW approaches, e.g. optPBE-vdW, optB86b-vdW, and optB88-vdW is absent in these studies.

In this work we first examine the influence of several vdW functionals on the structural and electronic properties of three common corundum-type sesquioxides, i.e. α-M_2O_3 with M $\in$ {Cr, Fe, Al}. These oxides have great technological significance. Chromium oxide is one of the most commonly used materials in technological applications as catalysts, corrosion resistance promotion, wear resistance, and stainless steel passivation layers [12,13]. Aluminum oxide has a wide variety of technological applications, ranging from catalysis to corrosion and adhesion. Due to its insulating properties, it is also adopted in microelectronic devices, i.e., field effect transistors, and integrated circuits [14]. α-Fe_2O_3 (known as hematite) is also used in many applications, such as oxidation catalysts, gas sensors and sorbents [15]. The (0001) surface of these oxides is the most stable surface and often occurs on naturally grown crystals.

[a] *Department of Physics, University of Antwerp, Groenenborgerlaan 171, B-2020 Antwerpen, Belgium*
[b] *Research Group PLASMANT, Department of Chemistry, University of Antwerp, Universiteitsplein 1, B-2610 Antwerp, Belgium.*
* E-mail: samira.dabaghmanesh@uantwerpen.be

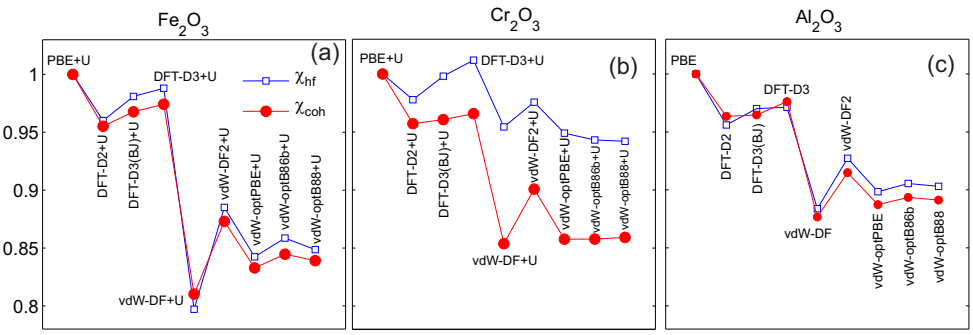

Fig. 1 (Color online)$\chi_{\rm coh}$ and $\chi_{\rm hf}$ (Eq.(3)) for α-Cr_2O_3, α-Fe_2O_3 and α-Al_2O_3 using different exchange correlation functionals.

As model systems to study the influence of vdW interactions on the adsorption of organic molecules on these surfaces we consider benzene and CH_3 molecules interacting with M_2O_3 substrates. This choice allows us to understand the influence of vdW corrections in both physisorption and chemisorption bonding. An important point in an adequate description of this adsorbate-surface interaction is a correct description of the bonding *within* the substrate. Furthermore, including nonlocal correlations in the study of solids may even improve the description of the cohesive properties [16]. For these reasons we first start with an investigation of the appropriateness of vdW functionals to describe the bulk properties of these oxides.

Our paper is organized as follows. In Sec. II we present the methods and formalisms used in our calculations. In Sec. III we present the results obtained for the bulk properties of M_2O_3 oxides. Our results for the adsorption energies of benzene and CH_3 follow in Secs. IV(A) and IV(B) respectively. Summary and conclusions are provided in Sec. V.

2 Methods

All density functional calculations in our work are carried out using the DFT code VASP (Vienna Ab-initio Simulation Package) [17,18]. The generalized gradient approximation (GGA) in the form of Perdew *et al.* [19] (PBE) was used to study the bulk and surface properties of the three considered metal oxides. Inspired by "Jacob's ladder" for vdW functionals [20], we start with the application of the most approximate vdW functionals to investigate the bulk properties, namely the vdW-Grimme[2] functionals which come in the forms of DFT-D2, DFT-D3-zero[3] and DFT-D3-BJ[21]. In these approaches the total energy of the system is given by

$$E_{\rm tot} = E_{\rm DFT} + E_{\rm dis} \qquad (1)$$

where $E_{\rm DFT}$ is the DFT total energy computed with a given exchange correlation functional. The dispersion interaction $E_{\rm dis}$ accounts for the missing long range interaction and has the asymptotic behavior of $-1/r^6$ at large particle distances r (see Eq. (11) in Ref. 2). These functionals differ in the way the prefactor of this asymptotic term is determined.

Next we apply vdW-inclusive functionals which should be, in principle, more general: the non-local vdW-density functionals vdW-DF (proposed by Dion *et al.* [1]) and vdW-DF2 (proposed by Murray *et al.* and Lee *et al.* [22,23]), as well as three optimized versions of the non-local vdW-DF functional, i.e. optB88-vdW, optB86b-vdW , and optPBE-vdW. The vdW-DF functional is directly based on the electron density in which the exchange correlation energy takes the form [16],

$$E_{xc} = E_x^{\rm GGA} + E_c^{\rm LDA} + E_c^{\rm nlc} \qquad (2)$$

where the exchange energy E_x^{GGA} uses the revPBE generalized-gradient approximation (GGA) functional, and E_c^{LDA} is the local density approximation (LDA) to the correlation energy. E_c^{nlc} is the non-local energy term which accounts approximately for the non-local electron correlation effects. The vdW-DF2 functional is an extended version of vdW-DF which aims to improve the binding description around energy minima in comparison to vdW-DF by changing both the exchange and nonlocal correlation components. In the optimized versions of vdW-DF, the exchange functional has been replaced by an optimized PBE (optPBE), optimized Becke88 (optB88-vdW), or optimized Becke86b (optB86b-vdW) to improve the accuracy of both vdW-DF (with the revPBE exchange) and vdW-DF2 (with rPW86 exchange) schemes. In order to correct the strong electronic correlation of the 3d-electrons of Cr and Fe in Cr_2O_3 and Fe_2O_3, the empirical PBE+U (with $U = 4$ eV, $J = 0.58$ eV [24] and $U = 5$ eV, $J = 1$ eV [25] respectively) are applied in the form proposed by Dudarev *et al.* [26]. In the presence of vdW functionals, we used DFT(vdW-DF/DF2/optPBE/optB88/optB86b)+U and (DFT-D2/D3)+U methods for α-Cr_2O_3 and α-Fe_2O_3 respectively. The combination of vdW functionals with DFT+U has already been applied in several works, e.g. in studying the adsorption

Table 1 Heat of formation (E_{hf}) and cohesive energy (E_{coh}) in eV, optimized lattice constants a and c, Cr-Cr, Cr-O bond lengths in Å, and magnetic moment μ in $\mu_B/atom$ of α-Cr_2O_3 bulk for different exchange-correlation functionals, PBE+U, and experimental values.

Method	E_{hf}	E_{coh}	a	c	μ	Cr-Cr/Cr-O
PBE+U	-13.34	-25.28	5.06	13.77	2.97	2.70/2.00
DFT-D2+U	-13.63	-26.39	5.04	13.56	2.96	2.69/1.98
DFT-D3-BJ+U	-13.36	-26.31	5.00	13.74	2.95	2.69/1.98
DFT-D3-zero+U	-13.39	-26.17	5.00	13.74	2.95	2.69/1.98
optB88-vdW+U	-12.55	-27.25	5.05	13.74	2.95	2.70/1.99
optB86b-vdW+U	-15.15	-27.17	5.03	13.67	2.94	2.68/1.98
optPBE-vdW+U	-15.80	-26.52	5.05	13.84	2.96	2.71/1.99
vdW-DF+U	-16.26	-25.105	5.12	13.91	2.98	2.74/2.02
vdW-DF2+U	-16.95	-25.94	5.13	13.91	2.98	2.76/2.02
Experiment	-11.76[34]	-26.87[35]	4.95[36]	13.56[36]	3.82[36]	2.623/1.96[36]

Table 2 Heat of formation (E_{hf}) and cohesive energy (E_{coh}) in eV, optimized lattice constants a and c, Fe-Fe, Fe-O bond lengths in Å, and magnetic moment μ in $\mu_B/atom$ of α-Fe_2O_3 bulk for different exchange-correlation functionals, PBE+U, and experimental values.

Method	E_{hf}	E_{coh}	a	c	μ	Fe-Fe/Fe-O
PBE+U	-9.08	-24.52	5.08	13.91	4.14	1.97/2.90
DFT-D2+U	-9.43	-25.65	5.07	13.62	4.13	1.94/2/90
DFT-D3-BJ+U	-9.24	-25.33	5.06	13.75	4.13	1.95/2.87
DFT-D3-zero+U	-9.19	-25.16	5.07	13.78	4.13	1.96/2.87
optB88-vdW+U	-6.84	-22.26	5.06	13.76	4.11	1.95/2.88
optB86b-vdW+U	-7.43	-23.42	5.04	13.69	4.10	1.95/2.86
optPBE-vdW+U	-6.28	-21.09	5.08	13.83	4.11	1.96/2.90
vdW-DF+U	-4.59	-17.98	5.130	14.05	4.13	1.98/2.94
vdW-DF2+U	-5.09	-17.99	5.15	14.12	4.09	1.98/2.97
Experiment	-8.56[34]	-25.17[37]	5.03[36]	13.75[36]	4.63[38,39]	1.95/2.89[40]

Table 3 Heat of formation (E_{hf}) and cohesive energy (E_{coh}) in eV, optimized lattice constants a and c, Al-Al, Al-O bond lengths in Å of α-Al_2O_3 bulk for different exchange-correlation functionals, PBE, and experimental values.

Method	E_{hf}	E_{coh}	a	c	Al-Al/Al-O
PBE	-15.12	-31.89	4.80	13.11	2.68/1.87
DFT-D2	-15.81	-31.73	4.78	13.01	2.66/1.86
DFT-D3-BJ	-15.58	-32.89	4.77	13.03	2.66/1.86
DFT-D3-zero	-15.57	-32.50	4.78	13.60	2.62/1.86
optB88-vdW	-13.79	-28.77	4.79	13.09	2.67/1.87
optB86b-vdW	-14.17	-31.29	4.78	13.06	2.66/1.86
optPBE-vdW	-12.91	-29.88	4.80	13.12	2.68/1.87
vdW-DF	-11.79	-27.93	4.83	13.20	2.70/1.88
vdW-DF2	-11.94	-28.58	4.85	13.25	2.72/1.88
Experiment	-17.04[41]	-31.83[42]	4.76[43]	12.98[43]	2.65/1.86[44]

of water on clean $CeO_2(111)$ surfaces[7], for water adsorption on rutile (110) surfaces[27], and for hydrogen activation, diffusion, and clustering on $CeO_2(111)$ surfaces[28]. In this work we employ the (DFT+U)+vdW approach for both the adsorption of molecules on the surfaces as well as for the bulk properties. This approach was recently also successfully applied to describe the structural and electrical properties of several transition metal oxides, hydroxides and oxyhydroxides.[29] Klimeš *et al.* tested the performance of non-local vdW functionals on the bulk properties of several elements and crystals using the DFT+vdW method[16].

For the calculation of the adsorption energies we use the optB86b-vdW(+U) functional from the non-local exchange correlation functionals and the DFT-D2(+U) method of Grimme. All vdW density functionals are used as implemented by Klimeš *et al.*[16] within the algorithm of Roman-Perez and Soler[30]. A plane wave cut-off of 500 eV and Monkhorst-Pack grid with 16×16×16, and 4×4×1 k-point grid determined by the Monkhorst-Pack method[31] were used to sample the Brillouin zone of the bulk and 2×2 supercell of the slabs, respectively. The vacuum gap thickness between periodic slabs is set to be $\sim$ 16 Å. The number of atomic layers along the z-axis of the clean slabs is kept in the range 13-15. It has been shown that the precision of the DFT calculations strongly depends on the number of relaxed layers of an oxide slab[32,33]. To avoid spurious electronic effects which may occur due to the non-relaxation of bottom layers of the slab we relax all substrate layers with a residual force threshold of 0.01 eV/Å. A dipole correction along the z-direction is used in the case of adsorption studies.

3 results and discussion

3.1 Bulk properties

α-Cr_2O_3, α-Fe_2O_3 and α-Al_2O_3 crystallize in the hexagonal corundum structure (space group $R\bar{3}c$), with six formula units in the bulk unit cell[45]. For nine different exchange correlation functionals we obtained the cohesive energy, equilibrium lattice constants, magnetic moment and bond lengths. The results are presented in Tables 1, 2 and 3. Both α-Cr_2O_3 and α-Fe_2O_3 are antiferomagnetic insulators. The antiferromagnetic order of the Cr and Fe layers along the [0001] direction is $+-+-$ for Cr_2O_3 and $++--$ for Fe_2O_3[25]. This magnetic ordering is found to be stable in all applied vdW functionals. It is clear from our results that the vdW functional has little influence on the magnetic moment.

Tables I, II and III show that all considered functionals overestimate the lattice constant and bond length values with respect to the experimental data. However, the vdW functionals slightly improve the structural properties over the PBE(+U) functional, except for the vdW-DF(+U) and vdW-DF2(+U) functionals, which is due to the fact that these two functionals are very repulsive at short interatomic distances. The largest differences with the experimental values for lattice parameters $a(c)$ are 0.18 Å(0.344 Å), 0.115 Å (0.37 Å), and 0.09 Å (0.27 Å), respectively for α-Cr_2O_3, α-Fe_2O_3 and α-Al_2O_3 in the case of vdW-DF2. These errors reduce to 0.08 Å (0.006 Å), 0.005 Å (0.06 Å), and 0.02 Å (0.08 Å) in the case of optB86b-vdW(+U), which confirms that the performance of this functional at short separations is better than the other non-local functionals.

Table I also shows that the different functionals give different cohesive energy values. Among the tested functionals, the vdW-DF and vdW-DF2 functionals are least accurate with respect to the experimental results (the maximum difference is found for α-Fe_2O_3, i.e. about 7 eV). This is due to the different structural parameters obtained using these functionals. Overall, the performance of the DFT-D2/D3 functionals are in better agreement with experiment than the optimized non-local functionals. This can be explained from the fact that in Eq. (1) the term E_{DFT} is obtained with the same, and clearly appropriate, PBE(+U) functional, while exchange functionals different from PBE(+U) are used for E_{xc} in Eq. (2). Among the non-local exchange correlation functionals, the optB86b-vdW(+U) functional shows the best agreement for the cohesive energy with experiment for the considered oxides. From the DFT-D family, we found that the DFT-D2(+U) method of Grimme yields the most accurate cohesive energy in α-Cr_2O_3 and α-Al_2O_3. Based on these results, we choose to calculate the adsorption energy using both the opt86b-vdW(+U) and DFT-D2(+U) functional in the next section.

The second column in Tables I, II and III shows our results for the heat of formation. There is a significant difference between the heat of formation energies obtained using the non-local density functionals with experiment and with those obtained within PBE(+U) and DFT-D for all three oxides. This discrepancy can be referred to the non-local density functional errors in the calculation of the total energy of both oxygen molecule and bulk oxide. For example, for the functionals optPBE-vdW(+U) and optB88-vdW(+U) $E_{hf}^{nlc} < E_{hf}^{DFT-D}$ in the case of α-Cr_2O_3 while this is opposite for α-Al_2O_3 and α-Fe_2O_3. Thus, in this case, an O_2 energy correction alone could not reduce the discrepancy for all three oxides. It is also instructive to investigate the contribution of the vdW interaction to the cohesive energy for these bulk materials for which the dispersion term should be small. We define the parameter $\chi_{\mathrm{coh/hf}}$ which determines the contribution of vdW interaction to the total cohesive energy, as the ratio

$$\chi_{\mathrm{coh/hf}} = \frac{E_{\mathrm{coh/hf}} - E_{\mathrm{coh/hf}}^{\mathrm{vdW}}}{E_{\mathrm{coh/hf}}} \qquad (3)$$

where $E_{\mathrm{coh/hf}}^{\mathrm{vdW}}$ is the cohesive energy/heat of formation that is

evaluated using the vdW contributions to the total energy.

Fig. 1 shows $\chi_{\mathrm{coh/hf}}$ for (a) α-Fe_2O_3, (b) α-Cr_2O_3, and (c) α-Al_2O_3 for the different exchange correlation functionals. In case of the PBE functional $\chi_{\mathrm{coh/hf}} = 1$ which is due to the absence of the vdW contribution. Clearly, our results distinguish the two different families of vdW functionals, i.e. DFT-D2/D3 and non-local methods. The results for E_{coh} of DFT-D2/D3 methods are closer to the PBE result compared to non-local vdW functionals just as E_{hf}. This highlights again the fact that the performance of the DFT-D2/D3 methods, resulting from E_{dis} in Eq. (1), are better in describing short separations compared to E_c^{nlc} in the non-local functionals (Eq. (2)).

3.2 Surface stability

There have been extensive theoretical and experimental studies on the (0001) surfaces of α-Cr_2O_3, α-Fe_2O_3, and α-Al_2O_3 due to their important applications as catalysts and substrates[46,47]. In these studies the clean surface[25,48–56] and adsorption properties of small molecules[57–63] were investigated.

For each metal oxide surface there are different possible terminations for the (0001) surface orientation. Low-energy electron diffraction[49] and scanning transmission microscopy[50] experiments indicate that under ultrahigh-vacuum conditions the α-Cr_2O_3 surface is terminated by a single layer of Cr with a bulk-like structure. Theoretical works have shown that depending on temperature and oxygen partial pressure, the surface may be either oxygen or chromyl (Cr=O) terminated[25,52]. In this work we study both the Cr and chromyl terminated (0001) surfaces. In the case of α-Fe_2O_3 Wang *et al.* [64] have shown that the Fe-terminated surface is stable under low oxygen pressure. Under O-rich conditions, the ferryl (Fe-O) terminated surface was found to be the most stable surface.[25] For the case of α-Al_2O_3, three main surface terminations are known: single and double Al terminated and oxygen terminated surfaces. We choose the non-polar Al-terminated surface in our adsorption study since this surface is found to be the most stable one[56,65–67]. Due to the instability of O-terminated surfaces of α-Al_2O_3[56] we do not consider the O-terminated surfaces here.

In the following we investigate the effect of these different terminations of the metal oxide surfaces on the adsorption properties of CH_3 and benzene. As the electronegativity of these surface atoms is very different for these surfaces we also expect the dispersion forces to be different.

3.3 Adsorption energies and geometries

To study the adsorption of benzene (as model system for physisorption) and CH_3 (as model for chemisorption), we rely on two different vdW-approaches, Grimme's DFT-D2(+U) and optB86b-vdW(+U), as motivated above. The adsorption energies on the (0001) were computed as

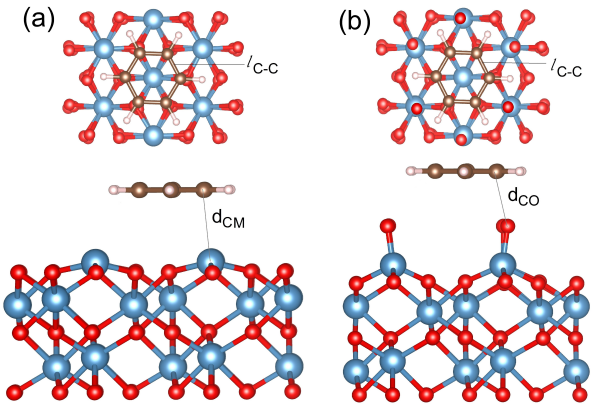

Fig. 2 (Color online) Adsorption of benzene on (a) Cr, Fe, and Al-terminated surfaces, (b) Cr-O and Fe-O terminated surfaces. Upper panel shows the top view and lower panel shows the side view of the molecule adsorbed on the surface.

$$E_{ads} = E_{mol-slab} - E_{mol} - E_{slab} \tag{4}$$

where $E_{mol-slab}$ is the total energy of the adsorbed molecule, E_{slab} is the total energy of the relaxed pure surface, and E_{mol} is the total energy of a relaxed gas-phase molecule in the same box used to compute the total system. The vdW contribution to the adsorption energy is calculated as follows:

$$E_{\mathrm{ads}}^{\mathrm{vdW}} = E_{\mathrm{mol-slab}}^{\mathrm{vdW}} - E_{\mathrm{mol}}^{\mathrm{vdW}} - E_{\mathrm{slab}}^{\mathrm{vdW}} \tag{5}$$

where $E^{vdW} = E^{nlc}$ and $E^{vdW} = E^{dis}$ are obtained using the non-local optB86b-vdW(+U) functional and the DFT-D2(+U) functional, respectively. The subindexes 'mol-slab', 'slab', and 'mol' indicate the considered system: adsorbed molecules, the relaxed bare oxides slab, and a relaxed gas-phase molecule. Using the lattice constants of the bulk metal oxide, we generated (2×2) supercell slabs with at least 16 Å vacuum in the z-direction. All atoms in the slab are free to relax during the structure relaxation.

3.3.1 Benzene adsorption The obtained adsorption energies of the benzene adsorption on the different terminations of the α-Cr_2O_3, α-Fe_2O_3 and α-Al_2O_3 (0001) surfaces are shown in Table 4. The adsorption geometries are given in Table 5 and the relaxed structures are illustrated in Fig. 2. The comparison between the adsorption energy and the vdW contribution to it is shown in Fig. 3.

In the case of metal-terminated surfaces, the interaction between the benzene and the surface is weak, and the vdW contribution results in a great enhancement of the adsorption energies with respect to PBE(+U). A key observation is that PBE(+U) yields negligible adsorption energies for all

Table 4 calculated adsorption energies in eV for benzene on different terminated surfaces of α-Cr_2O_3, α-Fe_2O_3, and α-Al_2O_3.

	α-Cr_2O_3		α-Fe_2O_3		α-Al_2O_3
Method	Cr	Cr-O	Fe	Fe-O	Al
PBE(+U)	-0.01	-2.04	-0.10	-1.09	-0.02
DFT-D2(+U)	-0.52	-2.43	-0.35	-1.10	-0.55
optB86b-vdW(+U)	-0.62	-2.55	-0.74	-1.14	-0.60

Table 5 Calculated $d_{CM/CO}$ (CM for metal terminated surfaces and CO for chromyl/ferryl terminated surfaces), l_{CC} in Å as defined in Fig. 2 (a,b) for benzene adsorbed on metal terminated surfaces as well as chromyl/ferryl terminated surfaces.

Method		Cr	Cr-O	Fe	Fe-O	Al
PBE(+U)	$d_{CM/CO}$	3.29	2.52	3.08	2.54	3.47
	l_{CC}	1.39	1.39	1.39	1.39	1.39
DFT-D2(+U)	$d_{CM/CO}$	2.68	2.23	2.63	2.13	2.82
	l_{CC}	1.39	1.40	1.39	1.39	1.39
optB86b-vdW(+U)	$d_{CM/CO}$	2.75	1.97	2.64	2.07	2.71
	l_{CC}	1.39	1.40	1.39	1.40	1.39

Table 6 calculated adsorption energies in eV for CH_3 on different terminated surfaces of α-Cr_2O_3, α-Fe_2O_3, and α-Al_2O_3.

	α-Cr_2O_3		α-Fe_2O_3		α-Al_2O_3
Method	Cr	Cr-O	Fe	Fe-O	Al
PBE(+U)	-1.60	-4.83	-1.16	-4.51	-0.79
DFT-D2(+U)	-1.78	-5.11	-1.31	-4.62	-1.09
optB86b-vdW(+U)	-1.93	-5.29	-1.67	-4.75	-1.18

Table 7 calculated $d_{CM/CO}$ and l_{CH} in Å as defined in Fig. 4(a,b) for CH_3 adsorbed on two terminated surfaces of α-Cr_2O_3, α-Fe_2O_3, and α-Al_2O_3.

Method		Cr	Cr-O	Fe	Fe-O	Al
PBE(+U)	$d_{CM/CO}$	1.99	1.45	2.01	1.39	2.08
	l_{CH}	1.09	1.09	1.09	1.10	1.09
DFT-D2(+U)	$d_{CM/CO}$	1.99	1.44	2.01	1.39	2.06
	l_{CH}	1.09	1.10	1.09	1.10	1.09
optB86b-vdW(+U)	$d_{CM/CO}$	1.99	1.43	1.99	1.38	2.05
	l_{CH}	1.10	1.10	1.09	1.10	1.09

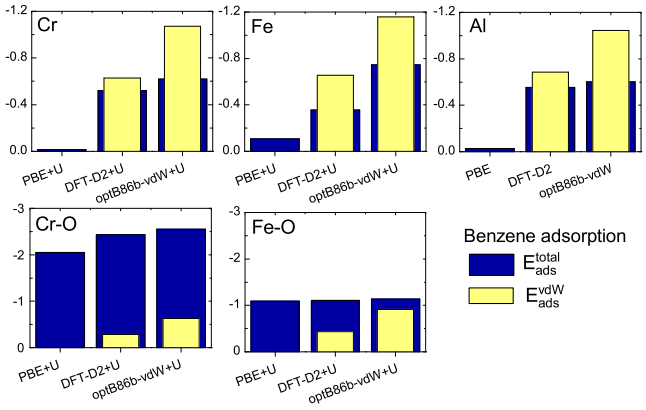

Fig. 3 (Color online) Total adsorption energies (thick blue bars) and E_{ads}^{vdW} (Eq.(5))(thin yellow bars) of benzene molecule adsorbed on the Cr, Fe, Al, Cr-O, and Fe-O terminated surfaces. Three different density functionals are considered: PBE(+U), DFT-D2(+U), and optB86b-vdW(+U).

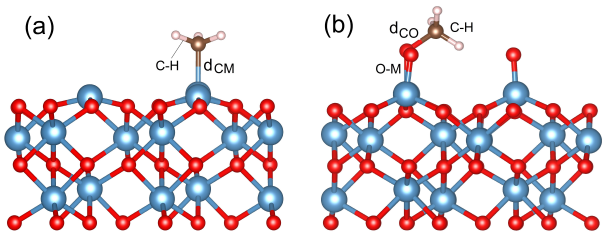

Fig. 4 (Color online) CH_3 molecule adsorbed on the (a) Cr, Fe, and Al terminated surfaces, (b) Cr-O and Fe-O terminated surfaces.

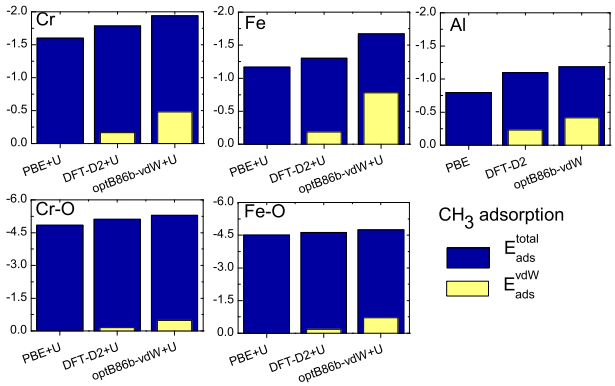

Fig. 5 (Color online) Total adsorption energies (thick blue bars) and E_{ads}^{vdW} (Eq. (5))(thin yellow bars) of CH_3 molecule adsorbed on the Cr, Fe, Al, Cr-O and Fe-O terminated surfaces. Three different density functionals are considered: PBE(+U), DFT-D2(+U), and optB86b-vdW(+U).

three metal-terminated oxides, while in contrast, the adsorption energies are significant for PBE(+U)+vdW. The adsorption of benzene on these metal terminated surfaces indeed corresponds to a physisorption type of attraction. We note that E_{ads}^{vdW} is larger than the total adsorption energy. These larger values of the vdW contribution (i.e. both E^{nlc} and E^{dis}) with respect to the total adsorption energies can be explained by the repulsive nature of the non-vdW terms which reduces the total adsorption energy after adding the vdW contribution (see Eq. (1) and (2)). Our results show that the inclusion of the vdW dispersion surmounts the PBE(+U) total adsorption energies up to 0.53 eV for the DFT-D2 in the case of the Al-terminated surface and 0.64 eV for the optB86b-vdW(+U) functional in the case of the Fe-terminated surface.

In case of the chromyl/ferryl terminations, one might also expect a weak physisorption for benzene. However, our results shown in the lower panels of Fig. 3 even show a much stronger adsorption compared to the metal terminated surfaces. This is due to the reactivity of oxygen atoms on top of the surface. In contrast to the adsorption on metal-terminated surfaces, the vdW contribution is smaller than the total adsorption energy. Larger E_{ads}^{total} and smaller d_{CO} compared to M-terminated surfaces (see Tables 4 and 5) suggest that the adsorption is thus more chemisorption-like. For this type of adsorption we obtained comparable values for the total adsorption energies with the vdW functionals as with the PBE(+U) functional. However, the differences in E_{ads}^{total} obtained using PBE(+U) and vdW functionals are still not negligible. This difference is up to 0.5 eV in the case of the optB86b-vdW(+U) functional for benzene adsorbed on the chromyl terminated surface. This energy difference indicates that vdW contributions are important even in chemisorption dominated adsorption. Comparing our results for the adsorption energy of benzene on metal terminated surfaces (see the lower panels in Fig. 3) we find smaller adsorption energies and larger vdW contributions for ferryl terminated compared to chromyl terminated surfaces. This means that the interaction of the benzene molecule with the ferryl terminated surface is weaker than with the chromyl terminated surface.

3.3.2 CH_3 adsorption In Fig. 5 we show the comparison between the adsorption energies and the vdW contribution to it for the adsorption of CH_3 on Cr, Fe, Al, Cr-O and Fe-O terminated surfaces. The adsorption energies are also listed in Table 6, the interatomic distances are listed in Table 7, and illustrated in Fig 4. For all investigated surfaces the vdW contribution E_{ads}^{vdW} is smaller than E_{ads}^{total}, which is due to the fact that the CH_3-M and CH_3-MO (M $\in$ {Cr, Fe, Al}) bonding is dominated by covalency. Although E_{ads}^{vdW} is much smaller than the total adsorption energy, the vdW correction in E_{ads}^{total} is still considerable. Our results show a difference in adsorption energy up to ~ 0.2 (~ 0.18) eV, ~ 0.51 (~ 0.15) eV, and

~ 0.39 (~ 0.3) eV for Cr/Fe/Al terminated surfaces in the case of optB86b-vdW(+U)(DFT-D2(+U)) functionals, in comparison to PBE(+U). The energy difference between E_{ads}^{vdW} and E_{ads}^{total} is larger in the adsorption of CH_3 on chromyl/ferryl terminated surfaces compared to Cr/Fe/Al terminated surfaces. This shows that the interactions between molecule and surface in chromyl/ferryl terminated surfaces are stronger than in the case of the metal terminated surfaces. These stronger interactions cause shorter C-O bonds, i.e. $\sim$1.45 Å for chromyl and $\sim$1.39 Å for ferryl terminated surfaces, compared to C-Cr ($\sim$1.99 Å), C-Fe ($\sim$2.01 Å) and C-Al ($\sim$2.08 Å) in metal terminated surfaces. Furthermore, the strong covalent bond between the methyl radical and the oxygen atoms in the surface, which leads to the small vdW correction, results in rather small relative changes in the total adsorption energies between the PBE+U and vdW approaches. In both benzene and CH_3 adsorption and for all examined surfaces, the optB86b-vdW(+U) functional yields to a larger adsorption energy than the DFT-D2(+U) approach.

3.3.3 Additional test using optPBE-vdW+U functional Finally, we note that the surface adsorption properties may differ from bulk properties, resulting in different behaviors of functionals in surface and bulk. Therefore we also test the performance of the optPBE-vdW+U functional, which is less promising in bulk, for the adsorption energies of CH_3 and benzene molecules on top of both Cr- and chromyl-terminated surfaces. Our results show that optPBE-vdW+U functional adsorption energies are in between the PBE+U results and those obtained using optB86b-vdW+U and DFT-D2+U functionals. The optPBE-vdW+U adsorption energies are $E_{ads}^{CH_3} = -1.70$ eV and $E_{ads}^{benzene} = -0.39$ eV for the Cr-terminated surface and $E_{ads}^{CH_3} = -4.85$ eV and $E_{ads}^{benzene} = -2.23$ eV for chromyl terminated surface.

4 Concluding remarks

Using the combination of PBE(+U) and two classes of vdW functionals (i.e. DFT-D and non-local density functionals) we have investigated the performance of different vdW methods by comparing the structural parameters, heat of formation, and cohesive energies of α-Cr_2O_3, α-Fe_2O_3, and α-Al_2O_3 bulk with experiment. Next, we adsorbed CH_3 and benzene molecules on top of different terminations of these oxides. We compared the computed adsorption energies and geometries using (DFT+U)-D2 and optB86b-vdW+U, with PBE+U in the case of α-Cr_2O_3, α-Fe_2O_3 and with PBE in the case of α-Al_2O_3. The vdW correction is essential for an accurate description of the bulk and adsorption properties of solids.

Our results for the bulk calculations demonstrate that among the examined functionals, DFT-D2(+U) (from the DFT-D based approach) and optB86b-vdW(+U) (from non-local correlation functionals) have the most accurate cohesive energies and lattice parameters compared to experiment. We found vdW-DF and vdW-DF2 functionals have the largest discrepancies for lattice parameters and cohesive energies. This indicates the importance of choosing an appropriate vdW functional in the study of metal oxides.

In the adsorption of benzene on top of Cr/Fe/Al terminated surfaces, as typical for physisorption, we found a significant increase in adsorption energies by including vdW contributions. Specifically, while PBE(+U) yields almost no adsorption energy, the vdW contributions increase the adsorption energies by $\sim 60\%$. In the adsorption of benzene on top of chromyl/ferryl terminated surfaces we found a chemisorption-like interaction. In this case, comparing the adsorption energies calculated by PBE(+U) with those including the vdW corrections demonstrate the importance of the vdW terms even for the strong interaction between the molecule and surface.

Adsorption of CH_3 on top of both surface terminations leads to chemisorption but even in the presence of such strong adsorption we found the vdW corrections to be not negligible. In both benzene and CH_3 adsorption and for all examined oxides, we found that optB86b-vdW(+U) functional yields a larger adsorption energy then the DFT-D2(+U) method. This indicates the more attractive nature of non-local vdW functionals in the studied metal oxides.

Acknowledgements. This work was supported by the Strategic Initiative Materials in Flanders (SIM). The computational resources and services used in this work were provided by the Vlaams Supercomputer Centrum (VSC) and the HPC infrastructure of the University of Antwerp.

References

1 M. Dion, H. Rydberg, E. Schroder, D. C. Langreth, and B. I. Lundqvist, *Phys. Rev. Lett.*, 2004, **92**, 246401 .
2 S. Grimme., *J. Comp. Chem.*, 2006, **27**, 1787 .
3 S. Grimme, J. Antony, S. Ehrlich, and S. Krieg, *J. Chem. Phys.*, 2010, **132**, 154104 .
4 J. Klimeš, D. R. Bowler, and A. Michaelides, *J. Phys.: Condens. Matter*, 2010, **22**, 022201 .
5 A. Tkatchenko, L. Romaner, O. T. Hofmann, E. Zojer, C. AmbroschDraxl, and M. Scheffler, MRS Bull., 2010, **35**, 435 .
6 J. Carrasco, W. Liu, A. Michaelides, and A. Tkatchenko, *J. Chem. Phys*., 2014, **140**, 084704 .
7 D. Fernandez-Torre, K. Kosmider, J. Carrasco, M. V. Ganduglia-Pirovano, *J. phys. Chem. C*, 2012, **116**, 13584-13593.
8 W. Liu, J. Carrasco, B. Santra, A. Michaelides, M. Schef-

fler, and A. Tkatchenkov, *Phys. Rev. B*, 2012, **86**, 245405 .
9 W. Liu, A. Tkatchenko, and M. Scheffler, Acc. Chem. Res., 2014, **47** (11), 33693377 .
10 S. D. Chakarova-Käck, Ø. Borck, E. Schröder, and B. I. Lundquist, *Phys. Rev. B*, 2006, **74**, 155402 .
11 P-A. Garrain, D. Costa, and P. Marcus, *J. phys. Chem. C*, 2011, **115**, 719-727.
12 M. P. McDaniel, *Adv. Catal.*, 1985, **33**, 47.
13 R. O. Adams, *J. Vac. Sci. Technol. A1*, 1983, **12**, 12-18 .
14 V. E. Henrich and P.A. Cox, *The Surface Science of Metal Oxides*, Cambridge: Cambridge University Press (1994).
15 X.-G. Wang, W. Weiss, S. K. Shaikhutdinov, M. Ritter, M. Petersen, F. Wagner, R. Schlogl, and M. Scheffler, *Phys. Rev. Lett*., 1998, **81**, 1038; T. Kendelewicz, P. Liu, C. S. Doyle, G. E. Brown, E. J. Nelson, and S. A. Chambers, *Surf. Sci*., 1999, **424**, 219 ; B. V. Reddy and S. N. Khanna, *Phys. Rev. Lett.*, 2004, **93**, 068301 .
16 J. Klimeš, D. R. Bowler, and A. Michaelides, *Phys. Rev. B*, 2011, **83**, 195131 .
17 G. Kresse and J. Hafner, *Phys. Rev. B*, 1993, **47**, 558.
18 G. Kresse and J. Furthmller, *Phys. Rev. B*, 1996, **54**, 11169.
19 J. Perdew, K. Burke, and M. Ernzerhof, *Phys. Rev. Lett*., 1996, **77**, 3865.
20 J. Klimeš, A. Michaelides, *J. Chem. Phys.*, 2012, **137**, 120901.
21 S. Grimme, S. Ehrlich, and L. Goerigk, *J. Comp. Chem*., 2011, **32**, 1456 .
22 E. D. Murray, K. Lee, and D. C. Langreth, *J. Chem. Theory Comput*., 2009, **5**, 2745.
23 K. Lee, E. D. Murray, L. Kong, B. I. Lundqvist, and D. C. Langreth, *Phys. Rev. B*, 2010, **82**, 081101.
24 N. Wu, A. L. Wysocki, U. Lanke, T. Komesu, K. D. Belashchenko, C. Binek, and P. A. Dowben, *Phys. Rev. Lett.*, 2011, **106**, 087202.
25 A. Rohrbach, J. Hafner, G. Kresse, *Phys. Rev. B*, 2004, **70**, 125426.
26 S. L. Dudarev, G. A. Botton, S. Y. Savrasov, C. J. Humphreys and A. P. Sutton, *Phys. Rev. B*, 1998, **57**, 1505.
27 N. Kumar, P. R. C. Kent, D. J. Wesolowski, and J. D. Kubicki, *J. Phys. Chem. C*, 2013, **117**, 23638-23644.
28 D. Fernandez-Torre, J. Carrasco, M. Veronica Ganduglia-Pirovano, and R. Perez, *J. Chem. Phys*., 2014, **141**, 014703.
29 Z. Zeng, M. K. Y. Chan, Z. Zhao, J. Kubal, D. Fan, and J. Greeley, *J. Phys. Chem. C*, 2015, **119**(32), 18177-18187.
30 G. Roman-Perez, J. M. Soler, *Phys. Rev. Lett*., 2009, **103**, 096102.
31 H. J. Monkhorst, J. D. Pack, *Phys. Rev. B*, 1976, **13**, 5188.
32 V. A. Ranea, I. Carmichael, and William F. Schneider, *J. Phys. Chem. C*, 2009, **113**, 2149-2158.
33 V. A. Ranea, William F. Schneider , and I. Carmichael, *Surface Science*, 2008, **602**, 268-275.
34 M. W. Chase, NIST-JANAF Thermochemical Tables 4th edn (Woodbury, NY: American Institute of Physics and American Chemical Society) (1998).
35 J. A. Cline, A. A. Rigos, and T. A. Arias, *J. Phys. Chem. B*, 2000, **104**, 6195.
36 L. Finger and R. Hazen, *J. Appl. Phys*., 1980, **51**, 5362.
37 M. Catti, G. Valerio, and R. Dovesi, *Phys. Rev. B*, 1995, **51**, 74417450.
38 J. Coey and G. Sawatzky, *J. Phys. C*, 1971, **4**, 2386.
39 E. Kren, P. Szabo, and G. Konczos, *Phys. Lett*., 1965, **19**, 103.
40 P. Canepa, E. Schofield, A. V. Chadwick, M. Alfredsson, *Phys. Chem. Chem. Phys*., 2011, **13**, 12826-12834.
41 D. Ghosh and D. A. R. Kay, *J. Electrochem. Soc*., 1977, **124**, 1836.
42 S. Hocker, P. Beck, S. Schmauder, J. Roth, and H. Trebin, *J. Chem. Phys*., 2012, **136**, 084707.
43 C. B. Alcock, Crystallograhic data on minerals, in CRC Handbook of Chemistry and Physics, 84th ed. edited by D. R. Lide (CRC Press, Boca Raton, FL, p. 4158. 33 (20032004)
44 R. E. Newnham and Y. M. de Haan, *Z. Kristallogr.*, 1962, **117**, 235.
45 L. Pauling and S. Hendricks, *J. Am. Chem. Soc.*, 1925, **47**, 781.
46 W. Geus, *Appl. Catal*., 1986, **25**, 313.
47 Alumina Chemical Science and Technology Handbook, edited by L.D. Hart (American Ceramic Society Inc., Westerville, OH, 1990).
48 C. Rehbein, N. M. Harrison, and A. Wander, *Phys. Rev. B*, 1996, **54**, 14066.
49 F. Rohr, M. Bäumer, H-J. Freund, J. A. Mejias, V. Staemmler, S. Muller, L. Hammer and K. Heinz, *Surf. Sci.*, 1997, **372**, L291.
50 V. Maurice, S. Cadot, and P. Marcus, *Surf. Sci.*, 2000, **458**, 195.
51 K. Wolter , D. Scarano , J. Fritsch , H. Kuhlenbeck , A. Zecchina, and H-J. Freund *Chem. Phys. Lett.*, 2000, **320**, 206.
52 X-G. Wang, and J. R. Smith, *Phys. Rev. B*, 2003, **68**, 201402.
53 S. A. Chambers, Y. J. Kim, and Y. Gao, *Surf. Sci. Spectra*, 1998, **5**, 219.
54 N. G. Condon, F. M. Leibsle, A. R. Lennie, P. W. Murray, T. M. Parker, D. J. Vaughan, and G. Thornton, *Surf. Sci.*, 1998, **397**, 278.
55 E. A. Soares, M. A. Van Hove, C. F. Walters, and K. F. McCarty, *Phys. Rev. B*, 2002, **65**, 195405.

56 X-G. Wang, A. Chaka, and M. Scheffler, *Phys. Rev. Lett.*, 2000, **84**, 3650.
57 T. Bredow, *Surf. Sci.*, 1998, **401**, 82.
58 M. Henderson, and S. A. Chambers, *Surf. Sci.*, 2000, **449**, 135.
59 M. Pykavy, V. Staemmler, O. Seiferth, and H-J, Freund, *Surf. Sci.*, 2001, **479**, 11.
60 O. Seiferth, K. Wolter, B. Dillmann, G. Klivenyi, H-J. Freund, D. Scarano, and A. Zecchina, *Surf. Sci.*, 1999, **421**, 176.
61 I. Hemmerich, F. Rohr, O. Seiferth, B. Dillmann, and H-J. Freund, *Z. Phys. Chem.*, 1997, **202**, 31.
62 Q. Guo, P. H. McBreen, and P. J. Moller, *Surf. Sci.*, 1999, **423**, 19.
63 D. Ta Thi, A. Kiet Tieu, H. Zhu, and B. Kosasih, *J. Phys. Chem. C*, 2015, **119**, 23.
64 X. G. Wang, W. Weiss, S. K. Shaikhutdinov, M. Ritter, M. Petersen, F. Wagner, R. Schlgl, and M. Scheffler, *Phys. Rev. Lett.*, 1998, **81**, 1038.
65 E. Wallin, J. M. Andersson, E. P. Münger, V. Chirita, and U. Helmersson, *Phys. Rev. B*, 2006, **74**, 125409.
66 K. C. Hass, W. F. Schneider, A. Curioni, and W. Andreoni, *J. Phys. Chem. B*, 2000, **104**, 5527.
67 J. Toofan, and P. R. Wilson, *Surf. Sci.*, 1998, **401**, 162.